Arteriosclerosis, Thrombosis, and Vascular Biology
JOURNAL OF THE AMERICAN HEART ASSOCIATION

Analysis of In Situ and Ex Vivo Vascular Endothelial Growth Factor Receptor Expression During Experimental Aortic Aneurysm Progression

Maureen M. Tedesco, Masahiro Terashima, Francis G. Blankenberg, Zoia Levashova, Joshua M. Spin, Marina V. Backer, Joseph M. Backer, Mien Sho, Eiketsu Sho, Michael V. McConnell and Ronald L. Dalman

Arterioscler. Thromb. Vasc. Biol. published online Jul 2, 2009;
DOI: 10.1161/ATVBAHA.109.187757
Arteriosclerosis, Thrombosis, and Vascular Biology is published by the American Heart Association. 7272 Greenville Avenue, Dallas, TX 72514
 Print ISSN: 1079-5642. Online ISSN: 1524-4636

Analysis of In Situ and Ex Vivo Vascular Endothelial Growth Factor Receptor Expression During Experimental Aortic Aneurysm Progression

Maureen M. Tedesco, Masahiro Terashima, Francis G. Blankenberg, Zoia Levashova, Joshua M. Spin, Marina V. Backer, Joseph M. Backer, Mien Sho, Eiketsu Sho, Michael V. McConnell, Ronald L. Dalman

Objective—Mural inflammation and neovascularization are characteristic pathological features of abdominal aortic aneurysm (AAA) disease. Vascular endothelial growth factor receptor (VEGFR) expression may also mediate AAA growth and rupture. We examined VEGFR expression as a function of AAA disease progression in the Apolipoprotein E–deficient (Apo $E^{-/-}$) murine AAA model.

Methods and Results—Apo $E^{-/-}$ mice maintained on a high-fat diet underwent continuous infusion with angiotensin II at 1000 ng/kg/min (Ang II) or vehicle (Control) via subcutaneous osmotic pump. Serial transabdominal ultrasound measurements of abdominal aortic diameter were recorded (n=16 mice, 3 to 4 time points per mouse) for up to 28 days. Near-infrared receptor fluorescent (NIRF) imaging was performed on Ang II mice (n=9) and Controls (n=5) with scVEGF/Cy, a single-chain VEGF homo-dimer labeled with Cy5.5 fluorescent tracer (7 to 18 μg/mouse IV). NIRF with inactivated single chain VEGF/Cy tracer (scVEGF/In, 18 μg/mouse IV) was performed on 2 additional Ang II mice to control for nonreceptor-mediated tracer binding and uptake. After image acquisition and sacrifice, aortae were harvested for analysis. An additional AAA mouse cohort received either an oral angiogenesis inhibitor or suitable negative or positive controls to clarify the significance of angiogenesis in experimental aneurysm progression. Aneurysms developed in the suprarenal aortic segment of all Ang II mice. Significantly greater fluorescent signal was obtained from aneurysmal aorta as compared to remote, uninvolved aortic segments in Ang II scVEGF/Cy mice or AAA in scVEGF/In mice or suprarenal aortic segments in Control mice. Signal intensity increased in a diameter-dependent fashion in aneurysmal segments. Immunostaining confirmed mural VEGFR-2 expression in medial smooth muscle cells. Treatment with an angiogenesis inhibitor attenuated AAA formation while decreasing mural macrophage infiltration and CD-31^{+} cell density.

Conclusion—Mural VEGFR expression, as determined by scVEGF/Cy fluorescent imaging and VEGFR-2 immunostaining, increases in experimental AAAs in a diameter-dependent fashion. Angiogenesis inhibition limits AAA progression. Clinical VEGFR expression imaging strategies, if feasible, may improve real-time monitoring of AAA disease progression and response to suppressive strategies. **(*Arterioscler Thromb Vasc Biol*. 2009;29:00-00.)**

Key Words: vascular endothelial growth factor ■ abdominal aortic aneurysms ■ imaging ■ neovascularization ■ angiogenesis inhibition

Abdominal aortic aneurysm (AAA) is a common and highly lethal age-associated vascular degenerative disease.[1] Characteristic pathological features present in both clinical and experimental aneurysms include marked elastin degradation and reduced medial vascular smooth muscle cell (SMC) cellularity in the presence of transmural inflammation and adventitial neovascularity. The exact sequence of and causal relationship between AAA-related pathological events, as well as the time-dependent expression of mural proinflammatory mediators during clinical disease progression, remain poorly understood.[2]

Although much emphasis has been placed on the consequences of medial SMC loss and matrix degeneration during aneurysm pathogenesis, the contribution of adventitial neovascularization to human disease progression appears increasingly significant. At the time of surgical repair, aneurysm tissue demonstrates increased mural neovascularization compared to nonaneurysmal aorta,[3] and rupture foci demonstrate increased neovascularity compared to intact aneurysm segments.[4] In experimental aneurysms, proangiogenic mediator expression correlates with transmural inflammation and AAA progression.[5–8] In an effort to evaluate the utility of mural neovascularity monitoring as a surrogate marker for disease progression we tested the ability of in situ and ex vivo near infrared fluorescent imaging (NIRF) to identify vascular endothelial growth factor receptor (VEGFR) expression in experimental AAAs.

Received March 8, 2009; revision accepted June 8, 2009.

From the Divisions of Vascular Surgery (M.M.T., M.S., E.S., R.L.D.), Cardiovascular Medicine (M.T., J.M.S., M.V.M.), and Nuclear Medicine (F.G.B., Z.L.), Stanford University Medical Center, Calif; and Sibtech Inc (M.V.B., J.M.B.), Brookfield, Conn.

Correspondence to Ronald L. Dalman.

Arterioscler Thromb Vasc Biol **is available at http://atvb.ahajournals.org** **DOI: 10.1161/ATVBAHA.109.187757**

Methods

Model Creation

All protocols were reviewed and approved by the Administrative Panel on Laboratory Animal Care at Stanford University (http://labanimals.stanford.edu/). C57/Bl 6 ApoE$^{-/-}$ mice, 11 to 14 weeks of age, weighing 25 to 30 g were anesthetized with inhaled isoflurane for surgical and imaging procedures and recovered with free access to food and water. Chronic subcutaneous angiotensin II (Ang II) infusion was used to create suprarenal murine AAAs.[9] After sterile preparation, osmotic mini-pumps (Alzet Model 2004, Durect Corporation, Cupertino) were inserted underneath the dorsal skin, delivering 1000 ng/kg/min Ang II (Sigma Lot 056K51001) in normal saline. Control mice received mini-pumps loaded with vehicle alone. After their procedures all mice were maintained on high-fat diets (40% kcal lipid, D12109, Resource Diets Inc) for up to 28 days. Using these methods, postoperative mortality was less than 10%.

Aortic Monitoring via Ultra-High Frequency Ultrasound

Transabdominal 40 MHz B-mode ultrasound (US) imaging was used to measure aortic diameter in vivo (supplemental Methods section, available online at http://atvb.ahajournals.org). Imaging was performed at intervals for up to 28 days after mini-pump implantation. Baseline suprarenal aortic diameter ranged from 0.8 to 0.85 mm; diameters >1.15 mm after Ang II infusion (>25% increase) were considered aneurysmal. Aortic diameters were measured in the longitudinal scan plane. Validation of US-determined aortic measurements using similar imaging protocols has been previously described.[10,11]

Fluorescence Imaging

At 21 to 28 days after mini-pump implantation, Ang II and Control mice underwent fluorescent imaging with scVEGF/Cy (Sibtech Inc), an engineered single chain (sc) VEGF homo-dimer, labeled with Cy5.5-maleimide (GE Healthcare) as previously described.[12] Additional Ang II mice received inactivated scVEGF/Cy (scVEGF/In) to control for nonreceptor-mediated intracellular accumulation (supplemental Methods section). Active or inactive scVEGF/Cy, 7 to 18 μg per mouse, was administered via penile vein injection approximately 2 hours before imaging sessions. After anesthetic induction, in vivo fluorescent images were obtained and analyzed via the Maestro NIRF Imaging System (Cambridge Research Instruments Inc). Four mice (2 Ang II scVEGF/Cy, 1 Control scVEGF/Cy, and 1 Ang II scVEGF/In) underwent additional fluorescent imaging with the eXplore Optix NIRF system (GE Healthcare). Postmortem in situ images were obtained after staged abdominal evisceration and subsequent bilateral nephrectomy. After the background signal was removed, scVEGF/Cy signal (signal) from regions of interest (ROI) within aneurysmal as well as grossly uninvolved distal aortic segments were calculated using respective system software. Fluorescent signal intensity reflects the counts per exposure time, normalized to area of ROI. The aortae were explanted and fixed immediately after in situ imaging. After aortic explantation, fixation and sectioning, ex vivo Cy5.5 fluorescence from representative aneurysmal and uninvolved aortic sections was confirmed using a 675/694 nm filtered Meiji MX6300 Fluorescence Microscope.

Angiogenesis Inhibition

After pump implantation, select mice were administered an angiogenesis inhibitor (Exel 0862, Exelixis Inc; 10 mg/kg daily, n=6), doxycycline (100 mg/kg, n=4), or vehicle alone (n=8), all by oral gavage, for 14 days. Mice were then euthanized for histological analysis as described above. Doxycycline is known to limit experimental AAA progression and was used as a positive control.[2] The IC50s (50% inhibitory concentration) of Exel 0862 were: FGFR1=3.7 nmol/L, FGFR2=3.5 nmol/L, Flt-1=13.6 nmol/L, KDR=2.4 nmol/L, PDGFRa=2.1 nmol/L, and PDGFRb=11.1 nmol/L. Exel 0862 has a bioavailability in mice of 52% and a half-life of 2.5 hours.

Tissue Preparation, Histological and Immunohistochemical Staining

Representative aneurysmal and nonaneurysmal aortic segments were selected for pressure perfusion fixation at 100 mm Hg with 4% PFA and embedded in paraffin. Aortic tissues were processed and embedded in paraffin. Blocks were sectioned at 4 μm for H&E and elastic Masson (EM) and immunohistochemical (IHC) staining. Sections were incubated for 1 hour at room temperature in primary antibody solutions including: (1) rabbit antimouse smooth muscle α-actin (SM-α) polyclonal antibody to stain for smooth muscle cells (1 μg/mL, Laboratory Vision); (2) rabbit antimouse CD31 polyclonal antibody to stain for endothelial cells (1 μg/mL, Laboratory Vision); (3) rat antimouse MAC-2 monoclonal antibody to stain for macrophages (0.5 μg/mL, Cedarlane); and (4) rabbit antimouse VEGFR-1 and VEGFR-2 polyclonal antibodies (1 μg/mL, Laboratory Vision) to stain for VEGF receptors. After staining with the primary antibodies, samples were incubated with the appropriate biotinylated secondary antibodies (Dako Inc & Biocare Medical) for 30 minutes at room temperature. Color development was performed using the DAB color development system (Dako Inc). For CD31/VEGFR-2, CD31/VEGFR-1, and SM-α/VEGFR- double staining, the DAB color development system (Dako Inc) was used for BrdU (brown color), and the Fast-red color development system (Biocare Medical) was used for GFAP (red color).

Statistical Analysis

Statistical analyses were performed with StatView (SAS) software. Data were expressed as mean±SE unless otherwise noted. Individual signal data were compared via 1-way ANOVA using the Fisher PLSD correction for multiple comparisons. The Pearson coefficient was used to calculate the correlation between aortic diameter and signal intensity. Differences were considered significant at $P<0.05$.

Results

VEGFR Signal Intensity Increases With Progressive Aortic Enlargement

Sixteen mice underwent NIRF fluorescence imaging with either scVEGF/Cy (9 Ang II, 5 Control) or scVEGF/In (2 Ang II). Because of intrinsic visceral and renal autofluorescence, AAA-specific signal was not discernable during transabdominal in vivo imaging. Therefore, subsequent signal acquisition and dosimetry calculations were obtained following evisceration and total nephrectomy (Figure 1). Using the Maestro system, signal intensity in aneurysmal aortic segments was significantly higher (0.342±0.045, mean±SE) than that obtained from remote nonaneurysmal segments in Ang II mice (0.160±0.048) and aortae from Control (0.091±0.043) and Ang II scVEGF/In mice (0.08±0.02, all $P<0.05$; Figure 2). Similar results were obtained using the eXplore Optix system on both whole vessel (supplemental Figure I) as well as tomographic aortic reconstructions (supplemental Figure II) from suprarenal aneurysms as well as noninvolved segments of the more distal aorta. Suprarenal aortic signal intensity correlated closely with US-determined aortic diameter obtained immediately prior to laparotomy (Figure 3).

Colocalization of Cy5.5 Fluorescence With VEGF Receptor Expression

Evidence for Cy5.5 colocalization (representing scVEGF/Cy uptake) within areas of VEGFR-2 expression identified by IHC was confirmed via fluorescence microscopy (Figure 4A and 4B). More Cy5.5 fluorescence and VEGFR-2 expression were present in aneurysmal as compared to nonaneurysmal aortic segments within the same animal (Figure 4C and 4D).

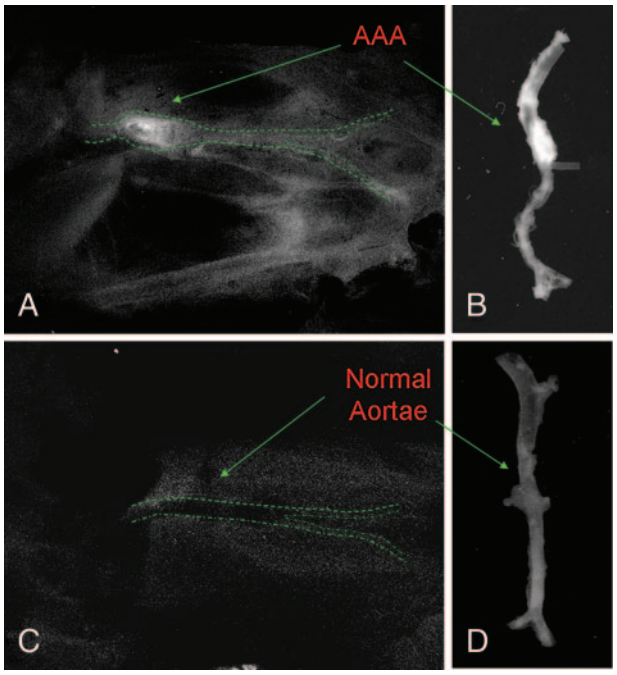

Figure 1. Fluorescence imaging with scVEGF/Cy tracer. A and B, In situ after abdominal evisceration and bilateral nephrectomies (A) and ex vivo (B) images of aneurysmal segments (arrows). C and D, In situ (C) and ex vivo (D) fluorescence images of control aorta at the suprarenal location (arrows). (Images A and C supine position with the head on the left; dotted lines outline aortic position).

Unexpectedly, maximal Cy5.5 fluorescence was evident in the best preserved, least involved regions of the aortic circumference within aneurysmal sections. No colocalization with VEGFR-2 expression was noted in scVEGF/In mice (Figure 4E and 4F).

VEGFR-2, VEGFR-1, and Neovascularization Within Aneurysmal Aortic Segments

Ang II aneurysmal aortic segments demonstrated characteristic regions of medial lamellar disruption (Figure 5A) and

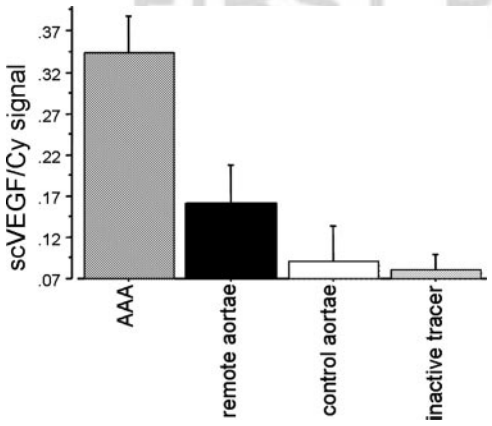

Figure 2. In situ fluorescence scVEGF/Cy signal of AAAs (n=9), remote segments of uninvolved (nonaneurysmal) aortae in AAA mice (n=9), control mice aortae (n=5), and mice injected with inactive scVEGF/Cy tracer (n=2). $P<0.05$ AAA vs remote (nonaneurysmal) aortae or control aortae or AAA with inactive tracer using 1-way ANOVA using the Fisher PLSD correction for multiple comparisons.

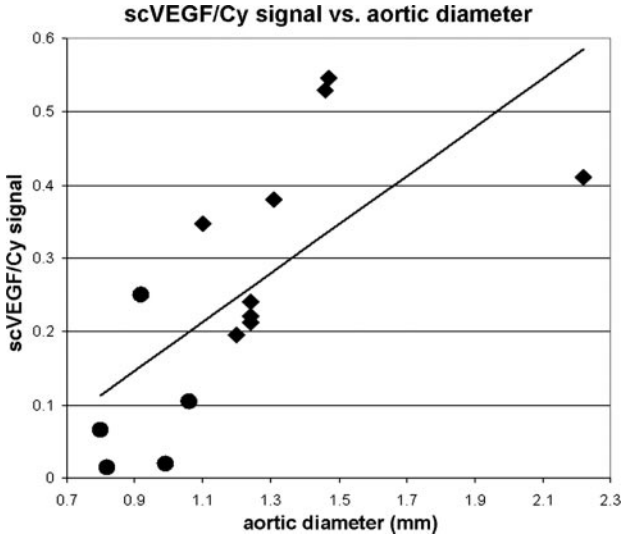

Figure 3. scVEGF/Cy suprarenal aortic signal from 9 AAA (squares) and 5 control mice (circles). Y=0.33, X−0.15, correlation coefficient $R=0.69$, $P=0.01$.

transmural mononuclear inflammation (Figure 5B) in isolated quadrants as previously described.[13] VEGFR-2 expression was evident circumferentially, and was most apparent in the areas of intact media within aneurysmal sections (Figure 5C). Costaining with smooth muscle α-actin confirmed maximal VEGFR-2 expression within medial smooth muscle cells (Figure 5D). Nonaneurysmal aortae from control and experimental mice demonstrated intact elastic lamellae, minimal inflammation and reduced VEGFR-2 expression (Figure 5E and 5F). Increased transmural VEGFR-1 expression was also present in aneurysmal aortic segments but was limited to the intima in nonaneurysmal aortae (supplemental Figure IIIA and IIIB).

Transmural neovessel formation was evident within aneurysmal segments as demonstrated by CD-31 immunostaining (Figure 6A). By comparison, few neovessels were present in nonaneurysmal aortic segments from either Ang II or Control mice (Figure 6B). Costaining studies of VEGFR-2 and CD-31 confirmed increased VEGFR-2 expression in areas of neovessel formation (Figure 6C). Within aneurysmal segments there was an abundance of adventitial neovessel formation in intact quadrants (Figure 6D) compared to limited constitutive cells and neovascularity present within disrupted regions (Figure 6E). CD-31 and VEGFR-1 costaining (supplemental Figure IIIC) also demonstrated the presence of VEGFR-1 expression in areas of adventitial neovascularization (supplemental Figure IIID).

Angiogenesis Inhibition Limits AAA Formation

Treatment with either Exel 0862 or doxycycline significantly decreased AAA diameter at 14 days compared to vehicle alone (Exel 0862 0.8±0.2 mm; Doxycycline 0.94±0.2 mm, Vehicle 1.3±0.2, $P<0.05$ Vehicle versus Exel 0862, Doxycycline). Aortae from both Exel 0862 and Doxycycline mice demonstrated decreased mural inflammation (Exel 0862 2.4±0.5 MAC-2 cells/high power field; Doxycycline 5.6±1.6; and Vehicle 36.8±8.5; $P<0.05$ Vehicle versus Exel 0862, Doxycycline). CD-31$^+$ cells (as a surrogate for neovascularity) were less prevalent in the Exel 0862 treated group versus all others. (Exel 0862 0.7±0.2 CD-31$^+$ cells/

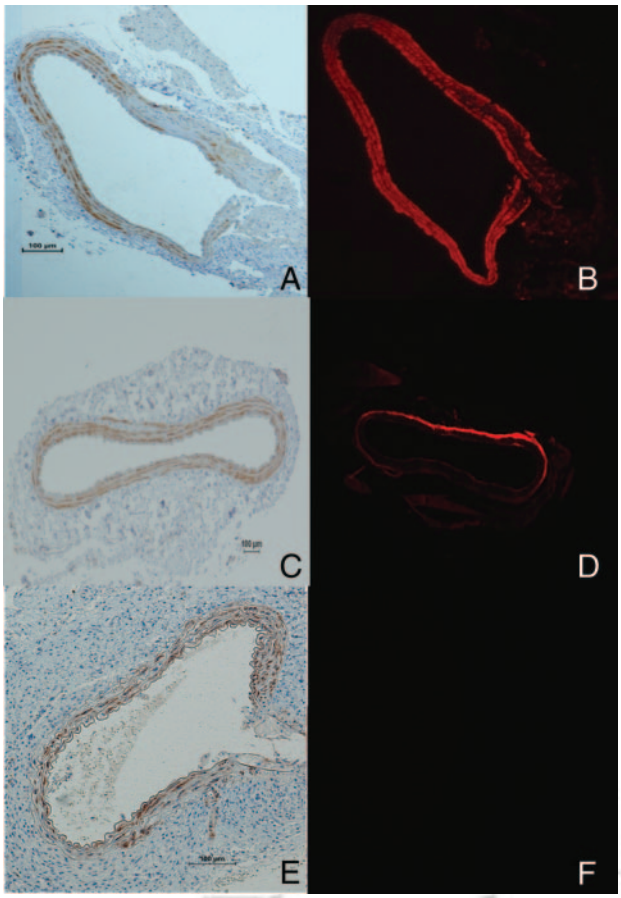

Figure 4. VEGFR-2 immunohistochemistry (left column) and Cy5.5 fluorescence microscopy representing VEGFR expression (right column) of representative AAA (A and B), remote segment (nonaneurysmal) aorta in an Apo $E^{-/-}$ mouse (C and D), and a AAA-injected with inactive tracer (E and F) at 10× magnification (scale bar=100 μm).

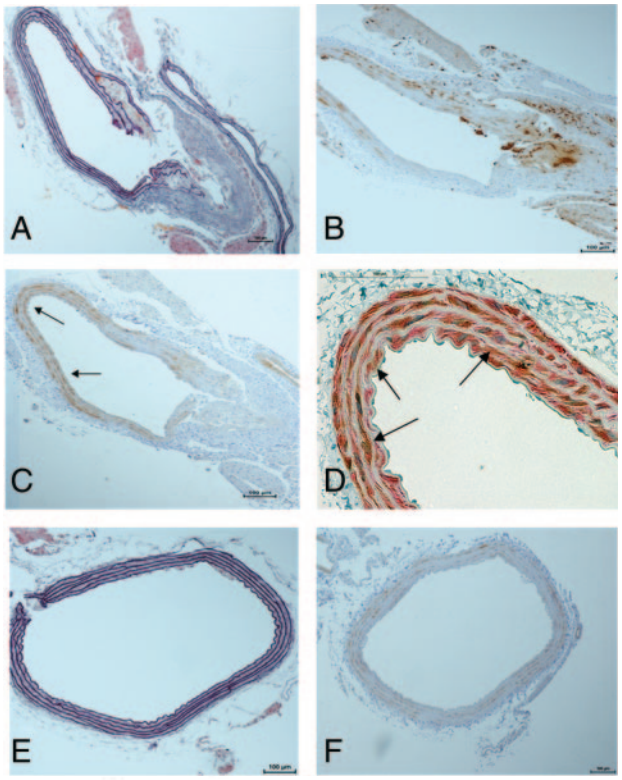

Figure 5. Histology of representative suprarenal AAA and nonaneurysmal aorta. A, Elastin Masson trichrome staining (10× magnification) highlights medial disruption characteristic of AAA. B, Transmural AAA inflammation demonstrated by MAC-2 staining (10× magnification). C, VEGFR-2 staining (10× magnification) in AAA tissue demonstrates increased expression (arrows) remote from areas of medial lamellar disruption. D, Colocalization (arrows) of smooth muscle alpha actin (red) and VEGFR-2 (brown; 40× magnification). E, Elastin Masson trichrome stain (10× magnification) of uninvolved nonaneurysmal aorta. F, Reduced VEGFR-2 staining (10× magnification) in nonaneurysmal aorta compared to AAA (C; scale bar=100 μm for all panels).

high power field; Doxycycline 10.4±3.5; and Vehicle 11.0±3.5; $P<0.05$ AI versus Vehicle, Doxycycline).

Discussion

In situ NIRF imaging with scVEGF/Cy consistently localized VEGFR expression to regions of concomitant aneurysmal degeneration in experimental AAAs. NIRF signal intensity correlated well with both aneurysm location and diameter. The fidelity of this colocalization was confirmed with ex vivo fluorescence microscopy. Both VEGFR-1 and 2 expression were increased within aneurysmal aortic segments. VEGFR-2 was most intensely expressed in medial smooth muscle cells in intact aortic medial segments adjacent to and across from sites of maximal inflammation and medial lamellar disruption. Similarly, CD31, as a surrogate for neovessel formation, was most abundantly expressed in intact adventitial segments with increased VEGFR-1 and 2 expression in proximity to areas of aneurysmal disruption. The mechanistic significance of neovessel formation in AAA progression was confirmed by profound reductions in mural inflammation and neovascularity after treatment with a broad-spectrum oral angiogenesis agent.

Mural neovascularization is recognized as a salient pathological feature of human AAA disease and may catalyze clinical progression.[3] Conversely, neovascularization may also play a role in protective or compensatory mural remodeling at other stages of human disease.[3,4,7,8,14,15] In our experimental construct, functional activity of VEGFR-1 as measured by scVEGF/Cy tracer uptake correlated well with aortic diameter. In addition, treatment with an angiogenesis inhibitor with competitive activity against VEGFR-1 and 2 as well as other vascular growth factor receptors significantly reduced mural inflammation and disease progression. Our data suggests that VEGFR expression and activity is mechanistically relevant to experimental AAA disease, and that VEGFR imaging may provide a useful window on disease progression.[16–23] If translatable to the human condition, these techniques or suitable alternatives may provide more accurate and timely guidance for suppressive medical therapies than absolute AAA diameter or growth rate alone.

Increased aortic VEGFR expression within aneurysmal segments was confirmed using 2 complementary fluorescence imaging systems as well as fluorescence microscopy and IHC. Although NIRF signal intensity correlated well with increasing aortic diameter, alternative explanations include both increased aortic tissue mass/wall thickness as well as

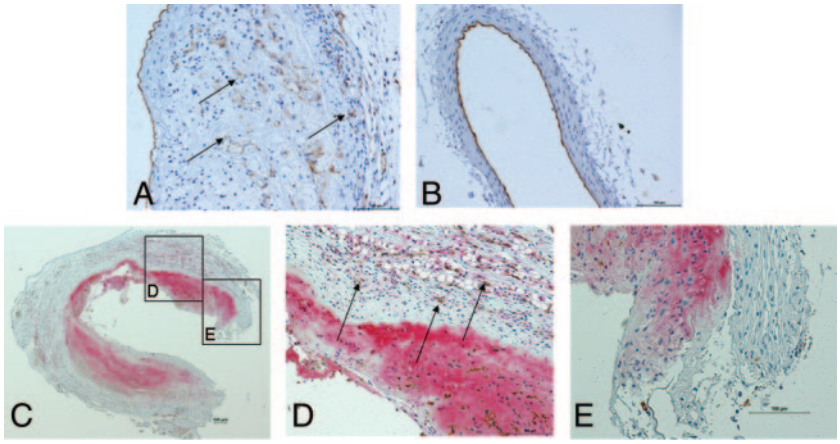

Figure 6. CD-31 immunohistochemistry of AAA tissue (A, 20× magnification) and nonaneurysmal aortic tissue (B, 20× magnification). Neovascularization is visualized throughout the AAA wall (A), as demonstrated by the CD-31$^+$ cells (arrows), but appears absent in nonaneurysmal segments (B). Double staining of CD-31 (brown) and VEGFR-2 (red) in AAA tissue (C, 4× magnification). Higher power magnification of the AAA in the area of the intact media demonstrates increased CD-31$^+$ cells (D, arrows, 20× magnification) in contrast to the disrupted wall of the aneurysm where there are few CD-31$^+$ cells (E, 20× magnification; scale bar=100 μm).

increased neovessel density per unit tissue. To control for intensity per unit area, tomographic in situ NIRF reconstructions were obtained in both axial and coronal planes. This technique confirmed increased signal intensity within aneurysmal planar sections, supporting our initial interpretation (eg, signal production reflected VEGF receptor expression per unit area).

Increased VEGFR-1 and 2 expression was present within aneurysmal aortic segments. VEGFR-1 was expressed in both the intima and adventitia; VEGFR-2 in the media and adventitia. VEGFR-2 colocalized to medial α-actin–positive cells. Although α-actin may not be expressed exclusively in differentiated vascular smooth muscle cells,[24] the marked regional localization of VEGFR-2 within the media strongly suggested SMC expression. Until recently VEGF and VEGFR were believed to be expressed exclusively by endothelial cells (ECs). Circulating endothelial progenitor cell populations are increased in AAA patients,[25] and VEGF is known to stimulate endothelial progenitor cell mobilization.[26] However, recent in vitro,[27,28] animal modeling,[29] and human tissue[30] studies demonstrate SMC VEGFR expression and migration in response to VEGF stimulation. Human and mouse embryonic stem cells differentiate into vascular smooth muscle cells that express VEGFR-2.[31] While vascular VEGFR-2 expression is minimal under quiescent conditions,[32] increased expression has been demonstrated in human and animal models of other disease states.[33,34] The presence of VEGFR-2 within human aortic smooth muscle cells in vitro has also been demonstrated.[35] The finding in the present study of maximal VEGFR-2 expression in aortic medial cells remote from areas of advanced inflammation and lamellar disruption was also unexpected, providing stimulus for further research into mechanisms for aneurysm initiation and localization in this model.

The relative paucity of both VEGFR-2 and CD-31$^+$ cells in disrupted mural quadrants may be a consequence of aortic dissection and contained rupture, both characteristic features of this AAA model. Imaging at earlier intervals may have revealed alternative expression patterns before medial disruption. Indeed, the cellular status of relatively intact quadrants adjacent to areas of medial disruption within aneurysmal segments are probably most representative of the relative neovascularity present in these areas just before medial disruption, and as such are more relevant to mechanisms involved in early disease progression.

Other limitations related to these modeling methods are well known and detailed elsewhere.[36] Confirming the timing, localization, and quantification of VEGFR expression in complementary AAA models may provide additional insights regarding the validity of these observations to human disease. The additional surgical exposure required for either the porcine pancreatic elastase infusion or abluminal calcium chloride application models will likely increase the total area of VEGFR expression present throughout the wound, however reducing the specificity and relevance of receptor localization and quantification for disease monitoring. The limited sensitivity of currently available transabdominal fluorescence imaging systems (in part because of intrinsic autofluorescence) made aortic exposure and evisceration necessary for adequate visualization. Proof of concept has clearly been established by this study, however, and further technical refinements may substantially improve efficacy and provide practical applications to human disease monitoring. Although tomographic imaging demonstrated increased tissue signal production per unit area, in practical terms the specificity of signal intensity as a function of tissue mass versus increased receptor expression is a secondary consideration because of the fact that enlarging aneurysms increase aortic tissue mass as a function of disease progression.

In conclusion, we demonstrate the feasibility of VEGFR expression imaging in experimental AAAs as a surrogate for disease progression. These findings lend further support to prior observations regarding the potential significance of VEGF, VEGF receptor activity, and medial and adventitial neovascularization in AAA pathogenesis. Similar or complementary molecular imaging strategies, if proven relevant to human disease, may expand diagnostic and therapeutic alternatives for AAA disease.

Acknowledgments

Both Mary Gerritsen PhD and Geoffrey Schultz MD made substantial contributions to the design and analysis of these experiments.

Sources of Funding

This work was supported by the National Institutes of Health (2 R01 HL064338-07, 2 RO1 EB000898-04, 2R44CA113080, 2R44CA113080), an American Heart Association Western States

Affiliate Postdoctoral Fellowship Award (0625171Y), Exelixis Inc, and GE Healthcare.

Disclosures

Marina Backer is an employee at Sibtech Inc, and Joseph Backer is the CEO of Sibtech Inc. Mary Gerritsen is an executive officer at Exelixis Inc.

References

1. Lederle FA, Johnson GR, Wilson SE, Chute EP, Littooy FN, Bandyk D, Krupski WC, Barone GW, Acher CW, Ballard DJ. Prevalence and associations of abdominal aortic aneurysm detected through screening. Aneurysm Detection and Management (ADAM) Veterans Affairs Cooperative Study Group. *Ann Intern Med*. 1997;126:441–449.
2. Thompson RW, Curci JA, Ennis TL, Mao D, Pagano MB, Pham CTN. Pathophysiology of abdominal aortic aneurysms: insights from the elastase-induced model in mice with different genetic backgrounds. *Ann N Y Acad Sci*. 2006;1085:59–73.
3. Paik DC, Fu C, Bhattacharya J, Tilson MD. Ongoing angiogenesis in blood vessels of the abdominal aortic aneurysm. *Exper Mol Med*. 2004; 36:524–533.
4. Choke E, Thompson MM, Dawson J, Wilson WRW, Sayed S, Loftus IM, Cockerill GW. Abdominal aortic aneurysm rupture is associated with increased medial neovascularization and overexpression of proangiogenic cytokines. *Arterioscler Thromb Vasc Biol*. 2006;26:2077–2082.
5. Crowther M, Goodall S, Jones JL, Bell PR, Thompson MM. Localization of matrix metalloproteinase 2 within the aneurysmal and normal aortic wall. *Brit J Surg*. 2000;87:1391–1400.
6. Crowther M, Goodall S, Jones JL, Bell PR, Thompson MM. Increased matrix metalloproteinase 2 expression in vascular smooth muscle cells cultured from abdominal aortic aneurysms. *J Vasc Surg*. 2000;32: 575–583.
7. Kobayashi M, Matsubara J, Matsushita M, Nishikimi N, Sakurai T, Nimura Y. Expression of angiogenesis and angiogenic factors in human aortic vascular disease. *J Surg Res*. 2002;106:239–245.
8. Sho E, Sho M, Nanjo H, Kawamura K, Masuda H, Dalman RL. Hemodynamic regulation of $CD34^+$ cell localization and differentiation in experimental aneurysms. *Arterioscler Thromb Vasc Biol*. 2004;24: 1916–1921.
9. Daugherty A, Manning MW, Cassis LA. Angiotensin II promotes atherosclerotic lesions and aneurysms in apolipoprotein E-deficient mice. *J Clin Invest*. 2000;105:1605–1612.
10. Barisione C, Charnigo R, Howatt DA, Moorleghen JJ, Rateri DL, Daugherty A. Rapid dilation of the abdominal aorta during infusion of angiotensin II detected by noninvasive high-frequency ultrasonography. *J Vasc Surg*. 2006;44:372–376.
11. Martin-McNulty B, Vincelette J, Vergona R, Sullivan ME, Wang Y-X. Noninvasive measurement of abdominal aortic aneurysms in intact mice by a high-frequency ultrasound imaging system. *Ultra Med Biol*. 2005; 31:745–749.
12. Backer MV, Levashova Z, Patel V, Jehning BT, Claffey K, Blankenberg FG, Backer JM. Molecular imaging of VEGF receptors in angiogenic vasculature with single-chain VEGF-based probes. *Nat Med*. 2007;13: 504–509.
13. Saraff K, Babamusta F, Cassis LA, Daugherty A. Aortic dissection precedes formation of aneurysms and atherosclerosis in angiotensin II-infused, apolipoprotein E-deficient mice. *Arterioscler Thromb Vasc Biol*. 2003;23:1621–1626.
14. Chapple KS, Parry DJ, McKenzie S, MacLennan KA, Jones P, Scott DJA. Cyclooxygenase-2 expression and its association with increased angiogenesis in human abdominal aortic aneurysms. *Ann Vasc Surg*. 2007;21: 61–66.
15. Choke E, Cockerill GW, Dawson J, Wilson RW, Jones A, Loftus IM, Thompson MM. Increased angiogenesis at the site of abdominal aortic aneurysm rupture. *Ann N Y Acad Sci*. 2006;1085:315–319.
16. Golledge J, Powell JT. Medical management of abdominal aortic aneurysm. *Eur J Vasc Endovasc Surg*. 2007;34:267–273.
17. Duftner C, Seiler R, Dejaco C, Fraedrich G, Schirmer M. Increasing evidence for immune-mediated processes and new therapeutic approaches in abdominal aortic aneurysms–a review. *Ann N Y Acad Sci*. 2006;1085: 331–338.
18. Rentschler M, Baxter BT. Pharmacological approaches to prevent abdominal aortic aneurysm enlargement and rupture. *Ann N Y Acad Sci*. 2006;1085:39–46.
19. Yoshimura K, Aoki H, Ikeda Y, Fujii K, Akiyama N, Furutani A, Hoshii Y, Tanaka N, Ricci R, Ishihara T, Esato K, Hamano K, Matsuzaki M. Regression of abdominal aortic aneurysm by inhibition of c-Jun N-terminal kinase. *Nat Med*. 2005;11:1330–1338.
20. Dawson J, Choke E, Sayed S, Cockerill G, Loftus I, Thompson MM. Pharmacotherapy of abdominal aortic aneurysms. *Curr Vasc Pharmacol*. 2006;4:129–149.
21. Thompson RW. Aneurysm treatments expand. *Nat Med*. 2005;11: 1279–1281.
22. Brady AR, Thompson SG, Fowkes FGR, Greenhalgh RM, Powell JT. Abdominal aortic aneurysm expansion: risk factors and time intervals for surveillance. *Circulation*. 2004;110:16–21.
23. Aoki H, Yoshimura K, Matsuzaki M. Turning back the clock: regression of abdominal aortic aneurysms via pharmacotherapy. *J Mol Med*. 2007; 85:1077–1088.
24. Owens GK, Kumar MS, Wamhoff BR. Molecular regulation of vascular smooth muscle cell differentiation in development and disease. *Physiol Rev*. 2004;84:767–801.
25. Dawson J, Tooze J, Cockerill G, Choke E, Loftus I, Thompson MM. Endothelial progenitor cells and abdominal aortic aneurysms. *Ann N Y Acad Sci*. 2006;1085:327–330.
26. Takahashi T, Kalka C, Masuda H, Chen D, Silver M, Kearney M, Magner M, Isner JM, Asahara T. Ischemia- and cytokine-induced mobilization of bone marrow-derived endothelial progenitor cells for neovascularization. *Nat Med*. 1999;5:434–438.
27. Ishida A, Murray J, Saito Y, Kanthou C, Benzakour O, Shibuya M, Wijelath ES. Expression of vascular endothelial growth factor receptors in smooth muscle cells. *J Cell Physiol*. 2001;188:359–368.
28. Grosskreutz CL, Anand-Apte B, Dupláa C, Quinn TP, Terman BI, Zetter B, D'Amore PA. Vascular endothelial growth factor-induced migration of vascular smooth muscle cells in vitro. *Microvasc Res*. 1999;58:128–136.
29. Ishida, Wu, Shi, Fujita, Sauvage, Hammond, Wijelath. Dynamic changes of smooth muscle and endothelial markers in the early healing process of dacron vascular grafts in the dog, using RT-PCR. *Int J Angiol*. 2000;9: 107–110.
30. Belgore F, Blann A, Neil D, Ahmed AS, Lip GYH. Localisation of members of the vascular endothelial growth factor (VEGF) family and their receptors in human atherosclerotic arteries. *J Clin Pathol*. 2004;57: 266–272.
31. Sone M, Itoh H, Yamahara K, Yamashita JK, Yurugi-Kobayashi T, Nonoguchi A, Suzuki Y, Chao T-H, Sawada N, Fukunaga Y, Miyashita K, Park K, Oyamada N, Sawada N, Taura D, Tamura N, Kondo Y, Nito S, Suemori H, Nakatsuji N, Nishikawa S-i, Nakao K. Pathway for differentiation of human embryonic stem cells to vascular cell components and their potential for vascular regeneration. *Arterioscler Thromb Vasc Biol*. 2007;27:2127–2134.
32. Witmer AN, Dai J, Weich HA, Vrensen GFJM, Schlingemann RO. Expression of vascular endothelial growth factor receptors 1, 2, and 3 in quiescent endothelia. *J Histochem Cytochem*. 2002;50:767–777.
33. Witmer AN, Blaauwgeers HG, Weich HA, Alitalo K, Vrensen GFJM, Schlingemann RO. Altered expression patterns of VEGF receptors in human diabetic retina and in experimental VEGF-induced retinopathy in monkey. *Invest Ophthalmol Visl Sci*. 2002;43:849–857.
34. Spliet WGM, Aronica E, Ramkema M, Witmer AN, Schlingemann RO, de Jong JMBV, Troost D. Immunohistochemical localization of vascular endothelial growth factor receptors-1, -2 and -3 in human spinal cord: altered expression in amyotrophic lateral sclerosis. *Neuropathol Appl Neurobiol*. 2004;30:351–359.
35. Chandra A, Angle N. Vascular endothelial growth factor stimulates a novel calcium-signaling pathway in vascular smooth muscle cells. *Surgery*. 2005;138:780–787.
36. Daugherty A, Cassis LA. Mouse models of abdominal aortic aneurysms. *Arterioscler Thromb Vasc Biol*. 2004;24:429–434.